Fabrication of a novel eco-friendly hybrid biocomosite based on carboxymethyl chitosan /polypropylene glycol /activated carbon for the highly efficient removal of Cr (III) from the aquatic medium: Adsorption, kinetic and antimicrobial evaluations

Eslam A. Mohamed (eslamazmy60@yahoo.com)
Egyptian Petroleum Research Institute
Amal A. Altalhi
Taif University College of Science
Nabel. A. Negm
Egyptian Petroleum Research Institute

Research Article

Keywords: Carboxymethylated chitosan, active carbon, chromium (III) remediation,antimicrobial activity

Posted Date: May 11th, 2022

DOI: https://doi.org/10.21203/rs.3.rs-1558232/v1

Abstract

Different nonionic biocomposite frameworks were prepared by supporting carboxymethylated chitosan polypropylene glycol on active carbon and characterized using sufficient characterization techniques. The prepared biocomposites comprised different modified chitosan to active carbon ratios. The biocomposites were achieved during remediation of chromium (III) ions from an aqueous medium. The influences of pH, chromium (III) ions concentration, time, and weight used in the remediation process were extensively studied to point out the optimized process conditions. The assigned optimum conditions of chromium (III) ions remediation were: 25 ^{o}C, using 0.6 g sorbents, and 100 ppm of ions concentration for 300 minutes at semi-neutral to neutral pH range of 6–7 to attain removal efficiency of 98.7%. The process was followed Freundlich adsorption isotherm and pseudo-second-order kinetics. The accumulation of ions onto biocomposites was regulated according to the intraparticle diffusion model, and the rate-determining step was the diffusion step. Increasing the active carbon-modified chitosan ratio in the biocomposites from 1:4 to 4:1, enhanced the remediation effectiveness of carboxymethylated chitosan in terms of equilibrium adsorption capacities increase from 67.93 mg/g to 70.25 mg/g. An opposing attitude was achieved by increasing the incorporated active carbon in the biocomposites during their antimicrobial efficacies assessments. The study presents a low-cost, eco-friendly, highly effective eliminator for highly contaminated aqueous media with Cr^{3+} ions. Furthermore, the prepared adsorbents exhibited high elimination efficiency in the presence of a high abundance of Cr^{3+} in the medium.

1. Introduction

The extensive utilization of heavy metals in industrial activities leads to a gradual rising in their ionic abundance in the activities drain water, which causes diverse ecological and health defects. Consequently, economic feasibility, sustainability, and effective remediation of various varieties of lethal contaminations have priority during ecological studies and research[1–3]. Chitin, chitosan, and agricultural wastes [4] are important substrates for remediation processes, which are ecofriendly and have the ability towards bio-deterioration [5]. During the removal of different pollutants from wastewater, including dyes, organics, metal ions, and drugs, chitosan represented marvel removal efficiency for all these pollutants[6, 7]. Chitosan is the second abundance biopolymer in nature that comes from the de-acetylation of chitin, the first abundant biopolymer in nature[8]. Chitosan lacks toxicity, is highly biocompatible, and has fast bio-deterioration; consequently, it attracted the attention of researchers for producing economically and efficiently modified adsorbents[9, 10]. Due to its superior characteristics, chitosan was modified to produce hydrogels with high swelling tendency, microcapsules, and microspheres, with enhanced mechanical and diffusion characteristics[11]. The motivating centers for chitosan adsorption tendencies are the amino (-NH_2), and hydroxyl (-OH) groups. These groups are not enough for presenting high adsorption tendencies for pure chitosan biopolymer, but chitosan always requires chemical modifications in its skeleton to present the required and expected efficiency[12, 13]. Several chemical modifications can be performed for pure chitosan to increase its susceptibility during adsorption. The modification processes include the introduction of glutaraldehyde[14, 15], glyoxal[16],

N,N-[bis(2-hydroxyl-3-formyl-5-methylbenzyl-dimethyl)]ethylene diamine[17], and ethylene glycol diglycidylether[18], in addition to carboxymethylation of chitosan to obtain caboxymthyl chitosan[19]. These derivatives contain hydroxyl (-OH), carboxyl (-COOH), amino (-NH_2) groups, which are good candidates for high adsorption efficiency.Active carbon is a natural product that can be produced from several processes including pyrolysis of biomass[20], charring of agricultural wastes, and chemical modification of organic wastes [21]. Active carbon can be used in wastewater treatment due to the presence of several active functional groups with high abundance which are mainly hydroxyl and carboxyl groups, in addition to some ester and carbonyl groups[22]. Wheat straw [23], waste biomass [24], seeds shells [25], and other agricultural products can be used as feedstock for the production of active carbon.Cr metal ions are presented in water sources in + 3, +5, and + 6 oxidation states, and the last is the most lethal form of them, due to its particular damages on DNA[26]. Among several applications: catalysts, glass production, and leather tanning used Cr^{3+}salts are extensivelyused.Nevertheless, Cr^{3+}effectively impacts some biological and metabolic processes, at which glucose level is increased in the cells. Hence, it was a necessity to establisha save protocol for the elimination of Cr^{3+}[27]. Among chemical oxidation [28], flocculation/coagulation [29], and biological remediation[30]; the adsorption method is regarded as a talented process for metal ions removal from contaminated water. This is due to its advantages including cost-effectively, easinessduring the application, the diversity of contaminants and pollutants which can be removed, high capacity during adsorption, and minimum produced sludge[31].In this study, carboxymethylated chitosan polypropylene glycol-active carbon biocomposite was prepared using different active carbon ratios and characterized. The biocomposites were achieved in the removal of chromium (III) ions from an aqueous medium. The influences of pH, chromium (III) ions concentration, time, and weight used in the remediation process were extensively studied. The adsorption isotherm and kinetic models of the process was studied

2. Experimental Section

2.1 Materials

Chitosan (CHI, 20–100 mPa/s)waspurchased from Shaanxi Pioneer Biotech Co., Ltd. Chloroacetic acid, triethylamine, sodium hydroxide, 2-propyl alcohol, methyl alcohol, and sodium bicarbonate were procured from Sinopharma Chem. Co., CHINA. Propylene oxide and activated carbon were purchased from Henan Tianfu Chemical Co., Ltd,

2.2 Preparation of carboxymethyl chitosan

Carboxymethyl chitosan was prepared according to the reported methodology [32]. In a typical method, CHI (7.5 gram), and sodium hydroxide (10.13 gram) were suspended in a suitable amount of 2-propyl alcohol (225 mL), and the medium moved at room temperature for2 h. Alcoholic solution of chloroacetic acid (7.5 g) in 50 mL of 2-propyl alcohol was added portion-wise during 1 h, and the temperature then was raised to 60 ^{o}C for 3 h; followed by filtration and recrystallization of the product from 75% aqueous methyl alcohol, and dried overnight to obtain the carboxymethylated chitosan (CMCN), (Scheme 1).

2.3 The reaction of CMCN and propylene oxide

Dried CMCN (5 g) was swelled in 5% ethanolic solution of acetic acid for 3 h under stirring, and then the reaction medium was desiccated at 65^{o}C for one day. The produced chitosonium acetate product (5 g), propylene oxide (0.3 mol, 17.4 g), and triethylamine (1 mL) were charged into a 250 mL closed glass reactor and tightly closed, and agitated at 45 ^{o}C for 10 h. The reactor was cooled to room temperature and evacuated (0.5 atm) at 40 ^{o}C for 1 h to eliminate triethylamine and excess propylene oxide and weighted[32]. The product then was neutralized by washing with sodium bicarbonate solution (0.1 M/20 mL), and then the product was dried at 80 ^{o}C under vacuum for 4 h, (Scheme 1).

2.4 Formation of CMCN-PG/activated carbon biocomposite

CMCN/PG and activated carbon were swelled individually in deionized water for 4 h, at 40 ^{o}C. Then, the two suspensions were mixed in different weight percent ratios (1:4, 1:1, 4:1 CMCN/PG: AC) and agitated at 50 ^{o}C for 4 h, followed by ultrasonic treating for 2 min (50% strength, CP505, Cole-Parmer, USA) to obtain the dispersed CMCN-PG/AC[33]. The dispersed product was settled down and decanted several times from distilled water, followed by drying under vacuum at 80 ^{o}C for 24 h to obtain three biocomposites, designated as CMCN-PG-AC4, CMCN-PG-AC, and CMCN-PG4-AC (Scheme 1) corresponded to the weight ratio of CMCN-PG to activated carbon.

2.5 Adsorption experiment

Adsorption experiments were progressed for the adsorption of Cr^{3+} metal ions onto the prepared biocomposites to determine the various parameters which influence the adsorption efficiencies of the biocomposites. The determined parameters were: influence of process time, initial metal ion concentration, amount of processed biocomposite, and pH of the medium.

The amount of biocomposite: different weights of the prepared biocomposites (0.1, 0.2, 0.3, 0.4, 0.5, and 0.6 g) were dispersed individually mechanically in 100 mL of Cr^{3+} solution (100 ppm) for 120 min. *Process time*:0.6 gram of biocomposite disseminated in 100 mL of Cr^{3+} solution (100 ppm) for different durations (60, 120, 180, 240, 300, and 360 min). *Metal ion concentration*:0.6 gram of biocomposites disseminated in 100 mL of Cr^{3+} solution (50, 100, 150, 200, and 250 ppm) for 120 minutes. *pH*: 0.6 gram of each biocomposite disseminated in 100 mL of Cr^{3+} solution (100 ppm) at different pH values (4–9) for 120 min. Each run was progressed in a 200 mL vessel with a stirring rate of 150 rpm under the thermostated condition at 25 ^{o}C. After each run, the medium was filtered, and the filtrate was collected and stored, while the residual biocomposites were dried and kept for further analysis. The concentration of the residual Cr^{3+} ions was determined using atomic absorption spectroscopy (Agilent-220 FS Atomic Spectrophotometer, United States).

The removal percentage of the metal ions was calculated using Eq. 1:

$$\text{Removal\%} = \frac{C_o - C_e}{C_e} \times 100$$

1

C_o, C_e: initial and equilibrium concentrations of Cr^{3+} ions, respectively.

2.6 Adsorption isotherm

Adsorption equilibrium study was carried out using 0.5 g of biocomposite in 100 mL Cr^{3+} solution at different concentrations of 50–250 ppm, pH of 7, and mixing speed of 150 rpm for 300 min. Isotherm models of Langmuir[34], and Freundlich [35] were applied to the experimental data using Eqs. 2–3, respectively.

$$q_e = \frac{q_m.K_L.C_e}{1+K_L.Ce} \quad (2)$$

$$q_e = K_f.C_e^{1/n} \quad (3)$$

q_e and q_m ($mg.g^{-1}$): concentration of Cr^{3+} metal ions at equilibrium, the maximum adsorption capacity of biocomposites; K_L is the Langmuir constant ($L.mg^{-1}$); K_F, n: Freundlich constant, adsorption intensity, respectively.

2.7 Kinetic study

The adsorption kinetics was determined by considering the influence of the immersion time on the adsorption process. The investigationalstatistics were scrutinized considering pseudo-first-order, pseudo-second-order, and interparticle diffusion renderingEqns. 4–6, respectively[36, 37]. R^2 was judged during inspecting the suitability of the correct model designates the kinetic performances of the adsorption progression.

$$q_t = q_e\left(1 - e^{-k_1 t}\right) \quad (4)$$

$$q_t = \frac{k_2 q_e^2.t}{1+ k_2 q_e.t} \quad (5)$$

$$q_t = k_{int} t^{1/2} \quad (6)$$

k_1, k_2, t, k_{int} (min^{-1}, $g.mg^{-1}.min^{-1}$, min, $mg.g^{-1}.min^{1/2}$): rate constants of pseudo-first and -second order models, contact time, and interparticle diffusion rate constant, respectively.

2.8 Anti-microbial activity

The modified chitosan-activated carbon biocomposites were screened for their anti-microbial action using well-diffusion methodology[38], using *S. aureus, S. mutants, E. coli*, *P. aeruginosa*, and *K.pneumonia, C. Albicans*, and *A. Nigar*, as tested micro-organisms, while ampicillin and gentamicin

operated as standards for the used bacterial genera, and dimethyl sulfoxide as a diluent. CMCN-PG-AC4, CMCN-PG-AC, and CMCN-PG4-AC biocomposites were achieved at a dosage of 15 mg/mL.

3. Results And Discussion

3.1 Adsorbents characterization

3.1.a FTIR spectroscopy(Nicolet 6700, Thermoelectron, USA)

FTIR spectra of both two raw materials (chitosan, and activated carbon) were provided to determine the essential absorption bands of each one and were shown as follows: FTIR of chitosan bared the subsequent bands (Fig. 1): broad absorption band centered at 3425 cm^{-1} represented for OH and NH_2 stretching band[39]–[40]; stretching bands within 2870–2920 cm^{-1} resembled C-H bonds[41]; the skeletal vibrations of C-O-C stretching band at 1026 and 1072 cm^{-1}; $-CH_2-$ bending appeared at 1420 cm^{-1}; asymmetric stretching of the C-O-C bridge gotten around 1153 cm^{-1}; 1540, 1318 cm^{-1} C = O amide; 1650 cm^{-1} –C = O bending of –NH; 815 cm^{-1} C-O-C glycoside bridge[42].activated carbon analysis using FTIR spectroscopy showed five types of absorption bands as follows (Fig. 1): 3500 cm^{-1}, (2920 cm^{-1}, 2870 cm^{-1}), 1690 cm^{-1}, 1035 cm^{-1}, and 875 cm^{-1} corresponding to O-H stretching, symmetric and asymmetric stretching of aliphatic C-H, C = O of aldehyde groups, C-O-C of ether vibration, and C = C (alkenes), respectively [43, 44]. The reaction between chitosan and propylene oxide in the presence of chloroacetic acid revealed the formation of carboxymethyl chitosan polypropylene glycol polymer *(CMCN-PG)*. The formation of *CMCN-PG* was confirmed by the presence of similar absorption bands of chitosan with the relative increase in the intensities of the three bands at 1100 cm^{-1} corresponded to ether groups of the formed propylene glycol as the result of the grafting of propylene glycol units in the main structure of chitosan, and 2920 cm^{-1}, and 2870 cm^{-1} assigned for symmetric and asymmetric stretching bands of aliphatic C-H of polypropylene glycol units which increased by increasing the propylene glycol units[45]. Initially, the formation of carboxymethyl chitosan was confirmed by the presence of an intense absorption near 1734 cm^{-1} corresponding to the formed ester groups, which proved the methylation of chitosan *CMCN*(Fig. 1)[46]. The formation of the targeted carboxymethyl chitosan polypropylene glycol-activated carbon biocomposites (CMCN-PG4-AC, CMCN-PG-AC, and CMCN-PG-AC4) happened via interaction between the formed carboxymethyl chitosan-polypropylene glycol and the activated carbon and their chemical structures were confirmed via FTIR analysis. FTIR spectra of CMCN-PG-AC biocomposite (representative for the prepared biocomposites) (Fig. 1) showed a combination of the absorption bands of carboxymethyl chitosan polypropylene glycol and activated carbon. The essential absorption band of the aldehyde groups characterized the activated carbon was appeared at 1690 cm^{-1}, while the absorption band characterized the carboxymethyl chitosan polypropylene glycol appeared at 1735 cm^{-1}[19]. The two composites of CMCN-PG4-AC and CMCN-PG-AC4 showed similar absorption bands with different intensities, confirming the formation of their

expected chemical skeleton. The presented FTIR spectra confirmed the formation of CMCN-PG4-AC, CMCN-PG-AC, and CMCN-PG-AC4 biocomposites as shown in Scheme 1.

3.1.bSEM image(JEM-7500F, China)

SEM images of the chitosan and the prepared biocomposites were printed in Fig. 2. It is clear that chitosan has different particle forms ranging between 50 and 200 µm, also it can be seen the asymmetrical particles in the form of sheets, in addition to a smooth un-voided surface[47]. The formed biocomposites showed the presence of activated carbon aggregates on the surface of chitosan flakes[48]. As can be observed in Fig. 2, the gradual increase in the distribution of activated carbon in chitosan film from 1:4 to 1:1, and 4:1 (CMCN-PG4-AC, CMCN-PG-AC, and CMCN-PG-AC4) increases the crystal-like structures of the activated carbon[49].

3.1.c XRD spectra(Empyrean, Netherlands)

XRD patterns of chitosan, activated carbon, CMCN-PG-AC4, CMCN-PG-AC, and CMCN-PG4-AC biocomposites were obtained at 2θ of 5 to 80°. XRD patterns of chitosan showed two characteristic signals at 10^{o} and 20^{o}, which is following the XRD fingerprint reported in several reports[50, 51]. Activated carbon showed a high amorphous structure as represented[52] in Fig. 3. The prepared biocomposites showed the characteristic fingerprint patterns of chitosan at 10^{o}, and 20^{o}, but the crystallinity in terms of the intensities of the characteristic peaks was decreased gradually by increasing the amount of activated carbon in the biocomposites. That can be attributed to the amorphous structure of activated carbon, which affects the crystallinity of the chitosan crystalline structure[53]. Generally, the performances of adsorption by different sorbents depend on adsorptive active sites accessibility. The highly crystalline adsorbents have low adsorption efficiencies due to the low accessibility of their adsorptive active sites[54]. Herein, the crystallinity of the prepared biocomposites is decreased and consequently, it will be expected the adsorption efficiencies will increase. That is due to the high accessibility of the different adsorptive sites of chitosan and activated carbon.

3.2 Optimization of adsorption parameters

Figure 4 represents the adsorption efficiencies of Cr^{3+} metal ions from the aqueous medium onto different amounts of CMCN-PG-AC4, CMCN-PG-AC, and CMCN-PG4-AC biocomposites. As a general observation, the removal efficiency of Cr^{3+} from the aqueous solution is gradually increased by the gradual increase in the number of used adsorbents. That increase in the adsorptive performance can be ascribed to the increase in the effective adsorptive sites on the adsorbents by increasing their amounts in the medium. The maximum adsorption efficiency can be obtained in the presence of 0.6 g/L of the three adsorbents as reported in several reports[55, 56].

Figure 5 showed the influence of the immersion time during 6 hours on the adsorption of Cr^{3+} ions from the aqueous medium on CMCN-PG-AC4, CMCN-PG-AC, and CMCN-PG4-AC biocomposites (0.6 g/L). As obtained from the analysis results, the adsorption efficiency profile was rapidly increased at the initial

time of the process (1–2 h), and then the increment was decreased steadily after longer periods. The rapid increase in the adsorption efficiency can be ascribed for the different Cr^{3+} ions concentration gradient between the bulk and the aqueous solution and the high concentration of unoccupied adsorptive centers on the biocomposites surfaces. The steady decrease in the adsorption efficiencies of the biosorbents after longer periods can be ascribed to the partial occupation of the adsorptive sites and the decrease in Cr^{3+} ions concentration gradient between the solution bulk and the metal ions on the adsorbent's surface. The maximum adsorption efficiency of the three biocomposite adsorbents was pointed at 5 h [57].Increasing the contact time increases the hydration of the biocomposites by water molecules, which increases the surface area of the biocomposites. The increase in the surface area makes the adsorption sites more available or accessible for interaction by Cr^{3+}metal ions. Comparison between the reported equilibrium times of modified chitosan [58], and the studied biocomposites showed that the prepared biocomposites have fewer equilibrium times. That can be attributed to the presence of propylene glycol units within the biocomposites framework, which eases their hydration throughout hydrogen bonding formation by the aqueous medium.

The effect of the initial concentration of Cr^{3+}metal ions on adsorption efficiencies of CMCN-PG-AC4, CMCN-PG-AC, and CMCN-PG4-AC biocomposites was explored at the initial concentration of Cr^{3+}metal ions from 50–250 ppm. Adsorbent dosage, pH, temperature, and contact time were secured as 7, 25 ∘C, 0.6 g for 5 h, Fig. 6. The gradual increase in the concentration of Cr^{3+} metal ions in the medium has a gradual decreasing effect on the adsorption efficiencies, which can be attributed to the ratio between the adsorptive sites and the free metal ions in the medium. At lower Cr^{3+} ions concentration, the adsorption is occurred effectively (> 99%) due to the absence of competition between the free and bounded Cr^{3+} ions (in the medium, or on the adsorbents). While, at high Cr^{3+} ions concentration in the medium, the complete removal is decreased (less than 99%) due to the presence of competition between the adsorbed and free metal ions [59], and also due to the decrease in the unbounded adsorptive sites on the surface of the biocomposite adsorbents. The increase in Cr^{3+} ion concentration than 250 ppm exhibited low adsorption efficiency for the different adsorbents, hence the optimal initial metal ion concentration was determined at 100 ppm.

The influence of pH of the medium on Cr^{3+} ions adsorption using CMCN-PG-AC4, CMCN-PG-AC, and CMCN-PG4-AC biocomposites at the range of 4–10 were represented in Fig. 7, in terms of adsorption efficiency. Figure 7 represented three concluding points at the studied pH range 4–10. In an acidic medium (pH = 4–5), the adsorption efficiencies of CMCN-PG-AC4, CMCN-PG-AC, and CMCN-PG4-AC biocomposites were low, which can be ascribed for the protonation of the adsorption active sites. The protonation process occurred for CMCN-PG-AC4, CMCN-PG-AC, and CMCN-PG4-AC biocomposites by H^+ ions in an acidic medium decrease the available deprotonated sites which can adsorb Cr^{3+} from the medium. In neutral medium at pH = 6–7, the adsorption efficiency of Cr^{3+} using CMCN-PG-AC4, CMCN-PG-AC, and CMCN-PG4-AC biocomposites was increased considerably to reach its maximum value at pH = 6(Fig. 7). In an alkaline medium (pH = 8–10), a considerable decrease in the adsorption efficiencies of

the three biocomposite adsorbents upon increasing the alkalinity to 10. That behavior can be attributed to the charge of Cr^{3+}ionsin the medium, which mainly depends on the pH of the medium as represented, Eq. 7–11 [60]:

$$Cr \leftrightarrow Cr^{3+} \quad (7)$$

$$Cr^{3+} + H_2O \leftrightarrow Cr(OH)^{2+} + H^+ \quad (8)$$

$$Cr(OH)^{2+} + H_2O \leftrightarrow Cr(OH)_2^{1+} + H^+ \quad (9)$$

$$Cr(OH)_2^{1+} + H_2O \leftrightarrow Cr(OH)_3(aq.) + H^+ \quad (10)$$

$$Cr(OH)_3(aq.) + H_2O \leftrightarrow Cr(OH)_4^{1-} + H^+ \quad (11)$$

As represented from the above equations (Eqs. 7–11), the ionic form of Cr^{3+} ions is changed gradually by increasing the pH of the medium. Increasing the pH converted the Crions into the bi-positively charged hydroxyl ions ($Cr(OH)^{2+}$), further increase in the pH changed the formed ions in Eq. 8 into chromium mono-cation ($Cr(OH)_2^{1+}$). At higher alkalinity, the chromium ions will precipitate as insoluble chromium hydroxide, which changed into negatively charged tetrahydroxy chromium complex with a negative charge ($Cr(OH)_4^-$). The adsorption active sites presented on the prepared CMCN-PG-AC4, CMCN-PG-AC, and CMCN-PG4-AC biocomposites are the hydroxyl and amino groups which have partially negative charges due to the presence of the lone pairs of electrons on oxygen and nitrogen atoms of –OH, and $–NH_2$ groups. Consequently, decreasing the positive charges on the metal ions will decrease their adsorption on the negatively charged adsorptive sites. As presented from Eqs. 7–11, the positive charges on Cr^{3+} ions are gradually decreased by the gradual increase in the pH. At high pH = 9, the high decrease in adsorption efficiencies of CMCN-PG-AC4, CMCN-PG-AC, and CMCN-PG4-AC biocomposites can be accounted for by the formation of the negatively charged species ($Cr(OH)_4^-$) in the medium.

As represented from Figs. 4–7, the adsorption efficiencies of the prepared adsorbents are dependent on the ratio of the activated carbon to the carboxymethyl chitosan polypropylene glycol presented in the nanocomposites. The gradual increase in the ratio of the activated carbon to modified chitosan from 1:4 to 4:1 is gradually increasing the obtained adsorption efficiencies. That can be ascribed for the diverse functional groups presented in the activated carbon, which acted as adsorption sites for Cr^{3+} ions from the medium. Increasing the activated carbon ratio up to 4:1 obtained the maximum adsorption efficiency among the three prepared adsorbents. From the adsorption study results, the removal of Cr^{3+} ions was optimally obtained from their aqueous medium using 0.6 g/L of CMCN-PG-AC4 after 6 hours at pH of 6–7, in the presence of 100 ppm of Cr^{3+} to obtain the maximum adsorption efficiency at 98.1%.

3.3 Adsorption isotherms of the adsorption process

Plotting the Langmuir adsorption isotherm equation variables, i.e., C_e vs. C_e/q_e, and extracting the correlation coefficient of the data according to the equation of state showed that R^2 values were 0.7886, 0.9361, and 0.9488 (Fig. 8). These values were lower than the unity, which displays the disagreement of the data of the adsorption process by the Langmuir adsorption isotherm[61]. Consequently, the data of the adsorption process required another isotherm model which can hold the process variables, which is the Freundlich adsorption isotherm[62]. This model in contrast to the Langmuir adsorption isotherm considers the interaction between the adsorbed species on the adsorbent surface. The model suggests a profile between log C_e and log q_e, Fig. 9. The model includes two parameters, K_F, and n, which signify the number of ions at equilibrium attached to the adsorbents, while n indicates the strength of adsorption onto the adsorbents surface, Table 1.

Table 1
Freundlich isotherm parameters of Cr^{3+} adsorption on CMCN-PG-AC4, CMCN-PG-AC, and CMCN-PG4-AC biocomposites

Biocomposite	Equation	K_F	n	1/n	R^2
CMCN-PG4-AC	y = 1.9536x + 0.509	1.66	0.51	1.960	0.9994
CMCN-PG-AC	y = 1.2139x + 1.2179	3.38	0.82	1.219	0.9995
CMCN-PG-AC4	y = 0.9289x + 1.5509	4.72	1.08	0.926	0.9999

The equation of state of Freundlich adsorption isotherm, K_F as a constant, is represented in Eq. 3. The valuen indicated inTable 1 figures the strength of Cr^{3+} ions adsorption onto the three biocomposites are increased by increasing the concentration of the activated carbon in the biocomposite. That proves the positive impact of activated carbon on the adsorption tendencies of the carboxymethyl chitosan polypropylene glycol biopolymer. This was confirmed by the increase in the K_F values, which indicate the number of ions at equilibrium attached to the adsorbents, and reached the maximum for CMCN-PG-AC4 biocomposite. CMCN-PG4-AC biocomposite has the lowest activated carbon (4CMCN-PG:1AC molar ratio) showed the lowest ability to adsorb metal ions as the corresponding n value was the lowest (n = 0.51) and lowest adsorption capacity as indicated by K_F value (1.66). While, CMCN-PG-AC4 biocomposite (1CMCN-PG:4AC molar ratio) exhibited the strongest adsorption to Cr^{3+} metal ions on its surface regarding n = 1.08, and the highest adsorption capacity regarding K_F value = 4.72.As concluded from the data in Table 1, it can be informed that the adsorption of Cr^{3+} metal ions onto CMCN-PG-AC4, CMCN-PG-AC, and CMCN-PG4-AC biocomposites obeys Freundlich adsorption isotherm. That leads to describe the adsorption of Cr^{3+} metal ions are occurs with interaction (repulsive) between the adsorbed metal ions on the biocomposites surface. The numeral amounts of 1/n lower than 1 reflect high adsorption intensity and surface heterogeneity[63, 64]. The constant value of n in Cr^{3+} ion adsorption by CMCN-PG4-AC, CMCN-PG-AC, and CMCN-PG-AC4 biocomposites was decreased by increasing the abundance of activated carbon in the formed biocomposite.This can be ascribed to the gradual increase in the

heterogeneity, and consequently suggests the raising of the adsorption capacity of the adsorbents in the following order: CMCN-PG4-AC < CMCN-PG-AC < CMCN-PG-AC4.

3.4 Kinetic evaluation

The kinetic evaluation was achieved using 100 ppm of Cr^{3+} metal ions at pH 6, in the presence of 0.2 g of CMCN-PG-AC4, CMCN-PG-AC, and CMCN-PG4-AC biocomposites, at ambient temperature. The residual concentrations of Cr^{3+} ions in the medium after the adsorption process for different interval times (120, 180, 240, 300, and 360 minutes) were determined in ppm. Concentrations were fitted using different kinetic models including pseudo-first-, second-order, and intra-particle diffusion kinetic models.

Pseudo-first orders kinetic model

the equation of state of the pseudo-first-order kinetic model comprises several factors, e.g., q_e, q_t, and k_1 which indicated the concentration of Cr^{3+} at equilibrium, and after the time (t), and pseudo-first-order rate constant, in mg/g, mg/g, and (1/min) units, respectively.

Figure 10 represented the graphical presentation of the adsorption data according to the pseudo-first-order kinetic equation of state (Eq. 4).The adsorption data did not comply with the pseudo-first-order model due to the intersection of the profile line with the x-axis and deeper with more negative values. Analyzing the profile during the first stage of adsorption revealed that this model is applicable at the short time adsorption process. This was referred to as the highly unoccupied concentration of the adsorptive active sites at the biocomposites surfaces during the first stage of the adsorption process[65].

Pseudo-second order kinetic model

this model commonly can fit adsorption data of metal ions in the solutions, using its equation of state (Eq. 5), and the variables of the pseudo-first-order model, in addition to additional parameters describing the rate-determining step of the second-order process (k_2, $g.mg^{-1}/min$), and graphically illustrated in Fig. 11, as follows[66]

Evidently, in Table 2, R^2 varied within 0.9998 to 1 (≈ 1) illustrating the appropriateness of the model for explaining the kinetics of the process. Further, calculating q_e gave comparable values to the experimental values[67], (Table 2).

Table 2
Kinetic data of Pseudo-second order model (* rate constant)

Biocomposites	R^2	q_e (mg/g)		Intercept	k_2*
		Theoretical	Experimental		
CMCN-PG4-AC	0.9998	78.13	74.55	0.2952	$5.6x10^{-4}$
CMCN-PG-AC	0.9999	78.13	74.34	0.2519	$6.5x10^{-4}$
CMCN-PG-AC4	1	78.74	73.95	0.2028	$7.9x10^{-4}$

As reported for the Pseudo-second order kinetic model [68, 69] the validity of this model is covering the entire time range of the process, additionally, the adsorption of Cr^{3+} ions occurred via electrostatic interaction between the positively charged metal ions and the electron lone-pairs located in the functional groups of the adsorbents (adsorptive sites).

Intraparticle diffusion model: this model supposes that the adsorption on the porous adsorbents is achieved throughout several stages, which can be summarized in the following: migration of high strength region (solution bulk) to lower concentration gradient (adsorbents/medium interface), adsorbed species film formation, and finally the diffusion of adsorbed species into the different adsorbent pores to interact with the adsorptive sites. Additionally, the rate-determining step was suggested to be the intraparticle diffusion step, and k_{int}, the rate constant can be determined according to Eq. 6(k_{int}= constant related to intraparticle diffusion stage, mg/g $min^{1/2}$)[70]:

Figure 12 represented the relationship between the square root of adsorption process time and the adsorbed amount of Cr^{3+} ions at the time (t), which illustrates the intraparticle diffusion model equation. The profile shows three characteristic regions that corresponded to the adsorption stages of Cr^{3+} ions on CMCN-PG-AC4, CMCN-PG-AC, and CMCN-PG4-AC biocomposites. Several parameters were extracted for the two major regions of the profile (the first and the third regions) including correlation coefficients (R^2), rate constant of rate-determining step (K_{int}), and adsorption capacity at equilibrium (q_e), Table 3.

Table 3
Extracted parameters from intraparticle diffusion kinetic model

Region	Migration from high to low concentration gradient			Diffusion region		
Biocomposites	R^2	K_{int}	q_e	R^2	K_{int}	q_e
CMCN-PG4-AC	0.9999	0.9912	55.88	1	03176	67.90
CMCN-PG-AC	0.9962	0.9450	57.52	1	03176	68.30
CMCN-PG-AC4	0.9943	0.8790	59.45	1	02268	70.25

Analyzing the data in Table 3 represents the following: In the first region, R^2 alternatedbetween 0.9999 to 0.9943, and the equilibrium adsorption capacity is ranged between 55.88 and 59.45 mg/g. The obtained values of the first region were out of the experimental values, which cannot be considered the rate-determining step. The diffusion region showed a correlation coefficient equal to unity ($R^2 = 1$), and the equilibrium adsorption capacity (q_e) were ranged between 67.9 mg/g and 70.25 mg/g. These values are following the experimental values, indicating that the diffusion step is the rate-determining step. The obtained values of the equilibrium adsorption capacity can be ordered in the following sequence: 70.25 mg/g, 68.30 mg/g, and 67.90 mg/g, for CMCN-PG-AC4, CMCN-PG-AC, and CMCN-PG4-AC biocomposite. The upsurge values of q_e by rising the activated carbon ratio in the different biocomposites confirms the occurrence of a synergistic performance between the modified chitosan and the activated carbon during the adsorption process of Cr^{3+} ions from the medium.

3.5 Mechanism of CMCN-PG-AC4 biocomposites

The adsorption mechanism is defined by several elements such as functional groups, electric charge, and the structures of the adsorbent and adsorbate. The functional groups of the adsorbent and the structuring of the adsorbate are two of the most critical factors that influence adsorption mechanism. In the CMCN-PG-AC4 biocomposites, the presence of $-NH_2$ and -OH groups in chitosan creates active locations for hydrogen bonds with Cr3 + ions. As previously discussion (effect of pH part), Cr(III) ions can exist in a variety of forms depending on the pH. Investigation the highly uptake of Cr(III) ions was obtained at pH = 6. In order to have a better knowledge of the adsorption mechanism, the FT-IR analysis of the CMCN-PG-AC4 biocomposites before and after adsorption process of Cr(III). As shown in Fig. 13, after Cr(III) adsorption, two additional peaks at 782 and 950 cm-1 were observed, which can be attributed to the Cr-O asymmetric and stretching vibrations, respectively. The vanishing of Cr–O and Cr—O—Cr vibration peaks in the spectrum of CMCN-PG-AC4 biocomposites after Cr desorption process, suggest that the adsorption mechanism involving the electrostatic attraction between adsorbent and Cr(VI) anionic species (Zhang, Xia, et al., 2015; Zhao et al., 2010).

3.6 Regeneration and reusability of adsorbents

According to previous studies, the regeneration and reusability of adsorbentare the perfect indicators for the evaluation of their performance for practical industrial applications, Recycling studies were conducted under ideal adsorption conditions, and the solvents for Cr (III) desorption were NaOH (0.1 M) solutions. As shown in Fig. 14 after five cycles, the adsorption efficient of CMCN-PG-AC4, CMCN-PG-AC, and CMCN-PG4-AC biocomposites remained at about 83%, 81%, and 80% respectively for Cr (III) metal ions, The slight decrease in adsorption capacity may be due to the formation of stable complexs, metal hydroxides between CMCN-PG-AC4, CMCN-PG-AC, and CMCN-PG4-AC biocomposites and heavy metal ions. However, the adsorbent still showed great reusability, which is beneficial to its practical application in the field of heavy metal wastewater treatment.

3.7 Antimicrobial activity

The antimicrobial activities of CMCN-PG-AC4, CMCN-PG-AC, and CMCN-PG4-AC biocomposites were tested against Gram−ve bacteria (*E. coli, K. pneumonia*), Gram + ve bacteria (*S. aureus, S. mutans*), and Fungi (*C. Albicans, A. Nigar*), Table 4.It was reported that chitosan biopolymer has acceptable antimicrobial activities against several types of microorganisms [71]. The efficacy of chitosan was found to increase by increasing the degree of deacetylation [72]. The reports pointed out that the origin of its antimicrobial activity comes from the presence of the amino groups along with chitosan segments[73].

Table 4
Antimicrobial efficacies of CMCN-PG-AC4, CMCN-PG-AC, and CMCN-PG4-AC biocomposites

Sample	Microorganism					
	Gram −ve bacteria		Gram + ve bacteria		Fungi	
	E. coli	K. pneumonia	S. aureus	S. mutans	C. albicans	A. Nigar
CMCN-PG4-AC	16 ± 0.5	14 ± 0.5	22.3 ± 0.5	30 ± 0.5	12.3 ± 0.5	NA
CMCN-PG-AC	12 ± 0.5	11 ± 0.5	20 ± 0.5	29 ± 0.5	11.6 ± 0.5	NA
CMCN-PG-AC4	9 ± 0.5	6 ± 0.5	16 ± 0.5	26 ± 0.5	10.3 ± 0.5	NA
Gentamicin	27 ± 0.6	25 ± 0.5	NA	NA	NA	NA
Ampicillin	NA	NA	22 ± 0.5	30 ± 0.5	NA	NA
Nystatin	NA	NA	NA	NA	21 ± 0.5	20 ± 0.5

Various descriptions were proposed of the antimicrobial function of chitosan biopolymer. Most of them suggested an interaction between the cellular membrane of bacteria and the chitosan, which leads to an upsurge in cellular permeability[74]. This consequently resulted in leakage of cellular components outside or inside the cells. This leakage causes growth disturbances as a result of reducing oxygen consumption required for the biosynthesis of essential components inside cells such as carbohydrates, protein, lipids, nucleotides, and genes[75]. Finally, the synthesis of RNA and DNA will be decayed and,directly decrease the bacterial cells[76].Assessment of CMCN-PG-AC4, CMCN-PG-AC, and CMCN-PG4-AC biocomposites during the antimicrobial tests showed the presence of a regular trend in the efficiency variation, which was depending on the ratio of active carbon in each biocomposite. It was found that the gradual increase in the ratio of active carbon in the biocomposites decreases gradually the antimicrobial activities, Table 4. That was attributed to the variation of the chitosan ratio in each biocomposite, which has enhanced antimicrobial efficiency by increasing its concentration. This was following several published reports.

Conclusions

Chitosan was carboxymethylated and grafted by propylene oxide to obtain grafted carboxymethyl chitosan, then its biocomposites by activated carbon at different ratios of the latter were formed to achieve efficient adsorbents for Cr^{3+} ions. The composition and texture of the prepared biocomposites were determined and the porosity was increased by increasing the activated carbon ratio. The adsorption

experiments of Cr^{3+} from aqueous solutions revealed the effective role of activated carbon in the adsorption process. The adsorption of Cr^{3+} was increased by increasing the time, Cr^{3+} initial concentration, adsorbents amounts, and the ratio of activated carbon. The adsorption process obeyed Freundlich adsorption isotherm according to the Pseudo-second order kinetic model. The adsorption was preceded through three steps and the rate-controlling process was the diffusion of Cr^{3+} ions into the adsorbents. The optimal adsorption efficiency was found at 98.1% using 0.6 g of adsorbents after 6 hours in the presence of 100 ppm of Cr^{3+} ions concentration in pH 6–7.

Declarations

Acknowledgment

I would like to thank Taif University Researcher supporting project number (TURP-2020/243), Taif University, Taif, Saudi Arabia.

The authors declare no competing interests.

References

1. Azmy EAM, Hashem HE, Mohamed EA, Negm NA (2019) Synthesis, characterization, swelling and antimicrobial efficacies of chemically modified chitosan biopolymer. J Mol Liq 284:748–754. https://doi.org/https://doi.org/10.1016/j.molliq.2019.04.054
2. Zhang L, Zeng Y, Cheng Z (2016) Removal of heavy metal ions using chitosan and modified chitosan: A review. J Mol Liq 214:175–191. https://doi.org/https://doi.org/10.1016/j.molliq.2015.12.013
3. Zia Q, Tabassum M, Gong R, Li J (2019) A Review on Chitosan for the Removal of Heavy Metals Ions. J Fiber Bioeng Informatics 12:103–128. https://doi.org/10.3993/jfbim00301
4. Negm NA, Abubshait HA, Abubshait SA, Abou Kana MTH, Mohamed EA, Betiha MM (2020) Performance of chitosan polymer as platform during sensors fabrication and sensing applications. Int J Biol Macromol 165:402–435. https://doi.org/https://doi.org/10.1016/j.ijbiomac.2020.09.130
5. Sawaguchi A, Ono S, Oomura M, Inami K, Kumeta Y, Honda K, Sameshima-Saito R, Sakamoto K, Ando A, Saito A (2015) Chitosan degradation and associated changes in bacterial community structures in two contrasting soils, Soil Sci. Plant Nutr 61:471–480. https://doi.org/10.1080/00380768.2014.1003965
6. Keshvardoostchokami M, Majidi M, Zamani A, Liu B (2021) A review on the use of chitosan and chitosan derivatives as the bio-adsorbents for the water treatment: Removal of nitrogen-containing pollutants. Carbohydr Polym 273:118625. https://doi.org/https://doi.org/10.1016/j.carbpol.2021.118625

7. Abhinaya M, Parthiban R, Kumar PS, Vo D-VN (2021) A review on cleaner strategies for extraction of chitosan and its application in toxic pollutant removal. Environ Res 196:110996. https://doi.org/https://doi.org/10.1016/j.envres.2021.110996
8. Sirajudheen P, Poovathumkuzhi NC, Vigneshwaran S, Chelaveettil BM, Meenakshi S (2021) Applications of chitin and chitosan based biomaterials for the adsorptive removal of textile dyes from water — A comprehensive review. Carbohydr Polym 273:118604. https://doi.org/https://doi.org/10.1016/j.carbpol.2021.118604
9. Saheed IO, Oh WD, Suah FBM (2021) Chitosan modifications for adsorption of pollutants – A review. J Hazard Mater 408:124889. https://doi.org/https://doi.org/10.1016/j.jhazmat.2020.124889
10. Liu Y, Li L, Duan Z, You Q, Liao G, Wang D (2021) Chitosan modified nitrogen-doped porous carbon composite as a highly-efficient adsorbent for phenolic pollutants removal. Colloids Surf Physicochem Eng Asp 610:125728. https://doi.org/https://doi.org/10.1016/j.colsurfa.2020.125728
11. Li W, Wei H, Liu Y, Li S, Wang G, Guo T, Han H (2021) An in situ reactive spray-drying strategy for facile preparation of starch-chitosan based hydrogel microspheres for water treatment application. Chem Eng Process - Process Intensif 168:108548. https://doi.org/https://doi.org/10.1016/j.cep.2021.108548
12. Jaiswal S, Dutta PK, Kumar S, Chawla R (2021) Chitosan modified by organo-functionalities as an efficient nanoplatform for anti-cancer drug delivery process. J Drug Deliv Sci Technol 62:102407. https://doi.org/https://doi.org/10.1016/j.jddst.2021.102407
13. Azmana M, Mahmood S, Hilles AR, Rahman A, Bin Arifin MA, Ahmed S (2021) A review on chitosan and chitosan-based bionanocomposites: Promising material for combatting global issues and its applications. Int J Biol Macromol 185:832–848. https://doi.org/https://doi.org/10.1016/j.ijbiomac.2021.07.023
14. Machado TS, Crestani L, Marchezi G, Melara F, de Mello JR, Dotto GL, Piccin JS (2022) Synthesis of glutaraldehyde-modified silica/chitosan composites for the removal of water-soluble diclofenac sodium. Carbohydr Polym 277:118868. https://doi.org/https://doi.org/10.1016/j.carbpol.2021.118868
15. Khapre MA, Pandey S, Jugade RM (2021) Glutaraldehyde-cross-linked chitosan–alginate composite for organic dyes removal from aqueous solutions. Int J Biol Macromol 190:862–875. https://doi.org/https://doi.org/10.1016/j.ijbiomac.2021.09.026
16. Jawad AH, Norrahma SSA, Hameed BH, Ismail K (2019) Chitosan-glyoxal film as a superior adsorbent for two structurally different reactive and acid dyes: Adsorption and mechanism study. Int J Biol Macromol 135:569–581. https://doi.org/https://doi.org/10.1016/j.ijbiomac.2019.05.127
17. Vasconcelos H, Camargo T, Gonçalves N, Neves A, Fávere V (2008) Chitosan crosslinked with a metal complexing agent: Synthesis, characterization and copper(II) ions adsorption. React Funct Polym 68:572–579. https://doi.org/10.1016/j.reactfunctpolym.2007.10.024
18. Abdulhameed A, Jawad AH, AbdulKarim-Talaq M (2019) Synthesis of chitosan-ethylene glycol diglycidyl ether/TiO2 nanoparticles for adsorption of reactive orange 16 dye using a response

surface methodology approach. Bioresour Technol 293:122071. https://doi.org/10.1016/j.biortech.2019.122071

19. Abdel Hafez OM, Mohamed RR, Abou Kana MTH, Mohamed EA, Negm NA (2021) Treatment of industrial wastewater containing copper and lead ions using new carboxymethyl chitosan-activated carbon derivatives. Egypt J Chem. https://doi.org/10.21608/ejchem.2021.82163.4050
20. Duan D, Chen D, Huang L, Zhang Y, Zhang Y, Wang Q, Xiao G, Zhang W, Lei H, Ruan R (2021) Activated carbon from lignocellulosic biomass as catalyst: A review of the applications in fast pyrolysis process. J Anal Appl Pyrolysis 158:105246. https://doi.org/https://doi.org/10.1016/j.jaap.2021.105246
21. Wu C, Li L, Zhou H, Ai J, Zhang H, Tao J, Wang D, Zhang W (2021) Effects of chemical modification on physicochemical properties and adsorption behavior of sludge-based activated carbon. J Environ Sci 100:340–352. https://doi.org/https://doi.org/10.1016/j.jes.2020.08.005
22. Abdulrazak S, Hussaini K, Sani HM (2017) Evaluation of removal efficiency of heavy metals by low-cost activated carbon prepared from African palm fruit. Appl Water Sci 7:3151–3155. https://doi.org/10.1007/s13201-016-0460-x
23. Naeem MA, Imran M, Amjad M, Abbas G, Tahir M, Murtaza B, Zakir A, Shahid M, Bulgariu L, Ahmad I (2019) Batch and column scale removal of cadmium from water using raw and acid activated wheat straw biochar. Water (Switzerland) 11:1–17. https://doi.org/10.3390/w11071438
24. Lucaci AR, Bulgariu D, Ahmad I, Lisa G, Mocanu AM, Bulgariu L (2019) Potential use of biochar from variouswaste biomass as biosorbent in Co(II) removal processes, Water (Switzerland).11https://doi.org/10.3390/w11081565
25. Okieimen FE, Okieimen CO, Ojokoh FI (2005) Rubber seed shell carbon as sequestrant of heavy metals and organic compounds from aqueous solution. Indian J Chem Technol 12:181–186
26. Keshavarz M, Foroutan R, Papari F, Bulgariu L, Esmaeili H (2021) Synthesis of CaO/Fe2O3 nanocomposite as an efficient nanoadsorbent for the treatment of wastewater containing Cr (III). Sep Sci Technol 56:1328–1341. https://doi.org/10.1080/01496395.2020.1778727
27. Wu S, Chandra Sekar N, Tan SN, Xie H, Ng SH (2016) Determination of chromium(III) by differential pulse stripping voltammetry at a chitosan-gold nanocomposite modified screen printed electrode. Anal Methods 8:962–967. https://doi.org/10.1039/c5ay03291a
28. Tünay O (2010) Chemical Oxidation Applications for Industrial Wastewaters, https://doi.org/10.2166/9781780401416
29. Muruganandam L, Kumar MPS, Jena A, Gulla S, Godhwani B (2017) Treatment of waste water by coagulation and flocculation using biomaterials, IOP Conf. Ser Mater Sci Eng 263. https://doi.org/10.1088/1757-899X/263/3/032006
30. Singh A, Bahadur Pal D, Mohammad A, Alhazmi A, Haque S, Yoon T, Srivastava N (2021) Kumar Gupta, Biological Remediation Technologies for Dyes and Heavy Metals in Wastewater Treatment: New Insight, Bioresour. Technol 126154. https://doi.org/https://doi.org/10.1016/j.biortech.2021.126154

31. Mousavi J (2018) Adsorption of heavy metals (Cu 2 + and Zn 2+) on novel bifunctional ordered mesoporous silica: Optimization by response surface methodology. J Taiwan Inst Chem Eng 84. https://doi.org/10.1016/j.jtice.2018.01.010
32. He B, Zhang Y, Li B, Chen Y, Zhu L (2021) Preparation and hydrophobic modification of carboxymethyl chitosan aerogels and their application as an oil adsorption material. J Environ Chem Eng 9:106333. https://doi.org/https://doi.org/10.1016/j.jece.2021.106333
33. Wang W, Ni J, Chen L, Ai Z, Zhao Y, Song S (2020) Synthesis of carboxymethyl cellulose-chitosan-montmorillonite nanosheets composite hydrogel for dye effluent remediation. Int J Biol Macromol 165:1–10. https://doi.org/https://doi.org/10.1016/j.ijbiomac.2020.09.154
34. Abubshait HA, Farag AA, El-Raouf MA, Negm NA, Mohamed EA (2021) Graphene oxide modified thiosemicarbazide nanocomposite as an effective eliminator for heavy metal ions. J Mol Liq 327:114790. https://doi.org/https://doi.org/10.1016/j.molliq.2020.114790
35. Amer A, Sayed GH, Ramadan RM, Rabie AM, Negm NA, Farag AA, Mohammed EA (2021) Assessment of 3-amino-1H-1,2,4-triazole modified layered double hydroxide in effective remediation of heavy metal ions from aqueous environment. J Mol Liq 116935. https://doi.org/https://doi.org/10.1016/j.molliq.2021.116935
36. Ezzati R (2020) Derivation of Pseudo-First-Order, Pseudo-Second-Order and Modified Pseudo-First-Order rate equations from Langmuir and Freundlich isotherms for adsorption. Chem Eng J 392:123705. https://doi.org/10.1016/j.cej.2019.123705
37. Babapour M, Hadi Dehghani M, Alimohammadi M, Moghadam Arjmand M, Salari M, Rasuli L, Ahmad Khan N (2021) Adsorption of Cr(VI) from aqueous solution using mesoporous metal-organic framework-5 functionalized with the amino acids: Characterization, optimization, linear and nonlinear kinetic models. J Mol Liq 117835. https://doi.org/https://doi.org/10.1016/j.molliq.2021.117835
38. Elshaarawy RFM, Ismail LA, Alfaifi MY, Rizk MA, Eltamany EE, Janiak C (2020) Inhibitory activity of biofunctionalized silver-capped N-methylated water-soluble chitosan thiomer for microbial and biofilm infections. Int J Biol Macromol 152:709–717. https://doi.org/https://doi.org/10.1016/j.ijbiomac.2020.02.284
39. Farag AA, Mohamed EA, Sayed GH, Anwer KE (2021) Experimental/computational assessments of API steel in 6 M H2SO4 medium containing novel pyridine derivatives as corrosion inhibitors. J Mol Liq 330:115705. https://doi.org/https://doi.org/10.1016/j.molliq.2021.115705
40. Anwer KE, Farag AA, Mohamed EA, Azmy EM, Sayed GH (2021) Corrosion inhibition performance and computational studies of pyridine and pyran derivatives for API X-65 steel in 6M H2SO4. J Ind Eng Chem. https://doi.org/https://doi.org/10.1016/j.jiec.2021.03.016
41. Negm NA, Sayed GH, Yehia FZ, Dimitry OIH, Rabie AM, Azmy EAM (2016) Production of biodiesel production from castor oil using modified montmorillonite clay. Egypt J Chem 59:1045–1060. https://doi.org/10.21608/ejchem.2016.1551

42. Tantala J, Thumanu K, Rachtanapun C (2019) An assessment of antibacterial mode of action of chitosan on Listeria innocua cells using real-time HATR-FTIR spectroscopy. Int J Biol Macromol 135:386–393. https://doi.org/https://doi.org/10.1016/j.ijbiomac.2019.05.032
43. Altalhi AA, Mohammed EA, Morsy SSM, Negm NA, Farag AA (2021) Catalyzed production of different grade biofuels using metal ions modified activated carbon of cellulosic wastes. Fuel 295:120646. https://doi.org/https://doi.org/10.1016/j.fuel.2021.120646
44. Sadeek SA, Mohammed EA, Shaban M, Abou MTH, Negm NA (2020) Synthesis, characterization and catalytic performances of activated carbon-doped transition metals during biofuel production from waste cooking oils. J Mol Liq 306:112749. https://doi.org/10.1016/j.molliq.2020.112749
45. Ulu A, Birhanlı E, Köytepe S, Ateş B (2020) Chitosan/polypropylene glycol hydrogel composite film designed with TiO2 nanoparticles: A promising scaffold of biomedical applications. Int J Biol Macromol 163:529–540. https://doi.org/https://doi.org/10.1016/j.ijbiomac.2020.07.015
46. Hemming EB, Masters AF, Perosa A, Selva M, Maschmeyer T (2019) Single-step methylation of chitosan using dimethyl carbonate as a green methylating agent. Molecules 24:6–8. https://doi.org/10.3390/molecules24213986
47. Zeng J, Ren X, Zhu S, Gao Y (2021) Fabrication and characterization of an economical active packaging film based on chitosan incorporated with pomegranate peel. Int J Biol Macromol 192:1160–1168. https://doi.org/https://doi.org/10.1016/j.ijbiomac.2021.10.064
48. Forteza R, Nifas GN (2019) Synthesis of Activated Carbon /. Chitosan Composites and Expanded Graphite for Symmetric Supercapacitor
49. Cleary M (2019) Comparative Study of Adsorption of Dyes onto Activated Carbon and Modified Activated Carbon by Chitosan Impregnation. J Chem Inf Model 53:1689–1699
50. R.S.C.M.D Q, Antonino BRPL, Fook VADO, Lima RÍDF, Rached EPN, Lima RJDS, Lima CAP, Covas MVL, Fook (2017) Preparation and characterization of chitosan obtained from shells of shrimp (Litopenaeus vannamei Boone). Mar Drugs 15:1–12. https://doi.org/10.3390/md15050141
51. Kumari S, Rath P, Sri Hari Kumar A, Tiwari TN (2015) Extraction and characterization of chitin and chitosan from fishery waste by chemical method. Environ Technol Innov 3:77–85. https://doi.org/https://doi.org/10.1016/j.eti.2015.01.002
52. Shamsuddin MS, Yusoff NRN, Sulaiman MA (2016) Synthesis and Characterization of Activated Carbon Produced from Kenaf Core Fiber Using H3PO4 Activation. Procedia Chem 19:558–565. https://doi.org/10.1016/j.proche.2016.03.053
53. Mousavi-Qeydari SR, Samimi A, Mohebbi-Kalhori D, Ahmadi E (2021) A mesoporous melamine/chitosan/activated carbon biocomposite: Preparation, characterization and its application for Ni (II) uptake via ion imprinting. Int J Biol Macromol 188:126–136. https://doi.org/https://doi.org/10.1016/j.ijbiomac.2021.08.020
54. Grząbka-Zasadzińska A, Ratajczak I, Król K, Woźniak M, Borysiak S (2021) The influence of crystalline structure of cellulose in chitosan-based biocomposites on removal of Ca(II), Mg(II), Fe(III) ion in aqueous solutions. Cellulose 28:5745–5759. https://doi.org/10.1007/s10570-021-03899-3

55. Liu X, Zhao Y, Liu T-A, Zhang (2021) Review on preparation and adsorption properties of chitosan and chitosan composites, Polym. Bull. https://doi.org/10.1007/s00289-021-03626-9
56. https://doi.org/10.1155/2021/6681486
57. Kannamba B, Reddy KL, AppaRao BV (2010) Removal of Cu(II) from aqueous solutions using chemically modified chitosan. J Hazard Mater 175:939–948. https://doi.org/10.1016/j.jhazmat.2009.10.098
58. Sun S, Wang A (2006) Adsorption kinetics of Cu(II) ions using N,O-carboxymethyl-chitosan. J Hazard Mater 131:103–111. https://doi.org/https://doi.org/10.1016/j.jhazmat.2005.09.012
59. Kumar R, Sharma H, Vishwakarma M, Joshi S, Bhandari N, Kandpal ND (2020) Adsorptive Removal of Pb(II), Cu(II) and Cd(II) Ions onto Rubus ellipticus as Low-Cost Biosorbent. Asian J Chem 32:495–500. https://doi.org/10.14233/ajchem.2020.22361
60. Ziemniak SE, Jones ME, Combs KES (1993) Solubility behavior of titanium(IV) oxide in alkaline media at elevated temperatures. J Solut Chem 22:601–623. https://doi.org/10.1007/BF00646781
61. García-González A, Zavala-Arce RE, Avila-Pérez P, Rangel-Vazquez NA, Salazar-Rábago JJ, García-Rivas JL, García-Gaitán B (2021) Experimental and theoretical study of dyes adsorption process on chitosan-based cryogel. Int J Biol Macromol 169:75–84. https://doi.org/https://doi.org/10.1016/j.ijbiomac.2020.12.100
62. Freundlich H (1907) Über die Adsorption in Lösungen. Z Für Phys Chemie 57U 385–470. https://doi.org/doi:10.1515/zpch-1907-5723
63. Asuquo E, Martin A, Nzerem P, Siperstein F, Fan X (2017) Adsorption of Cd(II) and Pb(II) ions from aqueous solutions using mesoporous activated carbon adsorbent: Equilibrium, kinetics and characterisation studies. J Environ Chem Eng 5:679–698. https://doi.org/https://doi.org/10.1016/j.jece.2016.12.043
64. Wang T, Chen P, Li M, Luo X, Liu L, Zeng G, Jiang J, Huang K, Xu X, Li S, Jiang H (2019) Synthesis of La2(C2O4)3 nanoprisms decorated with Fe3O4@m(ZrO2-CeO2) nanospheres and their application for effective fluoride removal. J Chem Technol Biotechnol 94:3650–3660. https://doi.org/10.1002/jctb.6170
65. Ho YS, Mckay G (1998) a C Om Parison of C Hem Isorptio N Kinetic M Odels Applied To Pollutant Rem Oval on Various So Rbents,76
66. Ho YS, McKay G (1999) Pseudo-second order model for sorption processes. Process Biochem 34:451–465. https://doi.org/https://doi.org/10.1016/S0032-9592(98)00112-5
67. Hashem A, Fletcher AJ, Younis H, Mauof H, Abou-Okeil A (2020) Adsorption of Pb(II) ions from contaminated water by 1,2,3,4-butanetetracarboxylic acid-modified microcrystalline cellulose: Isotherms, kinetics, and thermodynamic studies. Int J Biol Macromol 164:3193–3203. https://doi.org/https://doi.org/10.1016/j.ijbiomac.2020.08.159
68. Crini G, Badot P-M (2008) Application of chitosan, a natural aminopolysaccharide, for dye removal from aqueous solutions by adsorption processes using batch studies: A review of recent literature. Prog Polym Sci 33:399–447. https://doi.org/https://doi.org/10.1016/j.progpolymsci.2007.11.001

69. Hasan M, Ahmad AL, Hameed BH (2008) Adsorption of reactive dye onto cross-linked chitosan/oil palm ash composite beads. Chem Eng J 136:164–172. https://doi.org/https://doi.org/10.1016/j.cej.2007.03.038
70. Varma AJ, Deshpande SV, Kennedy JF (2004) Metal complexation by chitosan and its derivatives: a review. Carbohydr Polym 55:77–93. https://doi.org/https://doi.org/10.1016/j.carbpol.2003.08.005
71. Raafat D, Sahl HG (2009) Chitosan and its antimicrobial potential - A critical literature survey. Microb Biotechnol 2:186–201. https://doi.org/10.1111/j.1751-7915.2008.00080.x
72. Kiang T, Wen J, Lim H, Leong K (2004) The effect of the degree of chitosan deacetylation on the efficiency of gene transfection. Biomaterials 25:5293–5301. https://doi.org/10.1016/j.biomaterials.2003.12.036
73. Atay HY (2020) Antibacterial Activity of Chitosan-Based Systems,
74. Badawy MEI, Rabea EI, Eid AR, Badr MM, Marei GIK (2021) Structure and antimicrobial comparison between N-(benzyl) chitosan derivatives and N-(benzyl) chitosan tripolyphosphate nanoparticles against bacteria, fungi, and yeast. Int J Biol Macromol 186:724–734. https://doi.org/10.1016/j.ijbiomac.2021.07.086
75. Altalhi A, Hashem H, Negm N, Mohamed E, Azmy E (2021) Synthesis, characterization, computational study, and screening of novel 1-phenyl-4-(2-phenylacetyl)-thiosemicarbazide derivatives for their antioxidant and antimicrobial activities. J Mol Liq 333:115977. https://doi.org/10.1016/j.molliq.2021.115977
76. Raafat D, Von Bargen K, Haas A, Sahl HG (2008) Insights into the mode of action of chitosan as an antibacterial compound. Appl Environ Microbiol 74:3764–3773. https://doi.org/10.1128/AEM.00453-08

Scheme

Scheme 1 is available in Supplementary Files section.

Figures

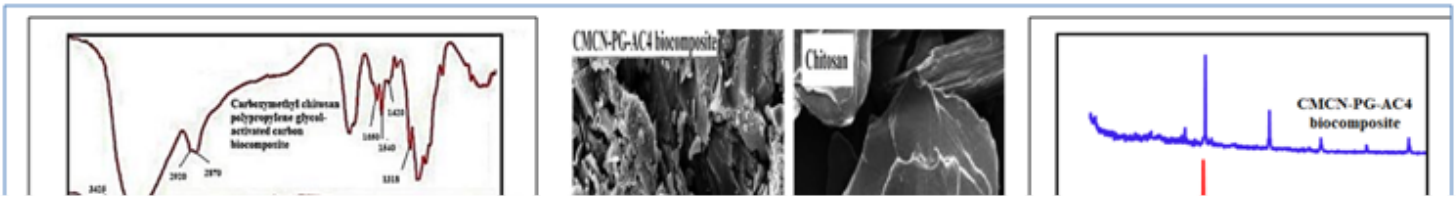

Figure 1

See image above for figure legend

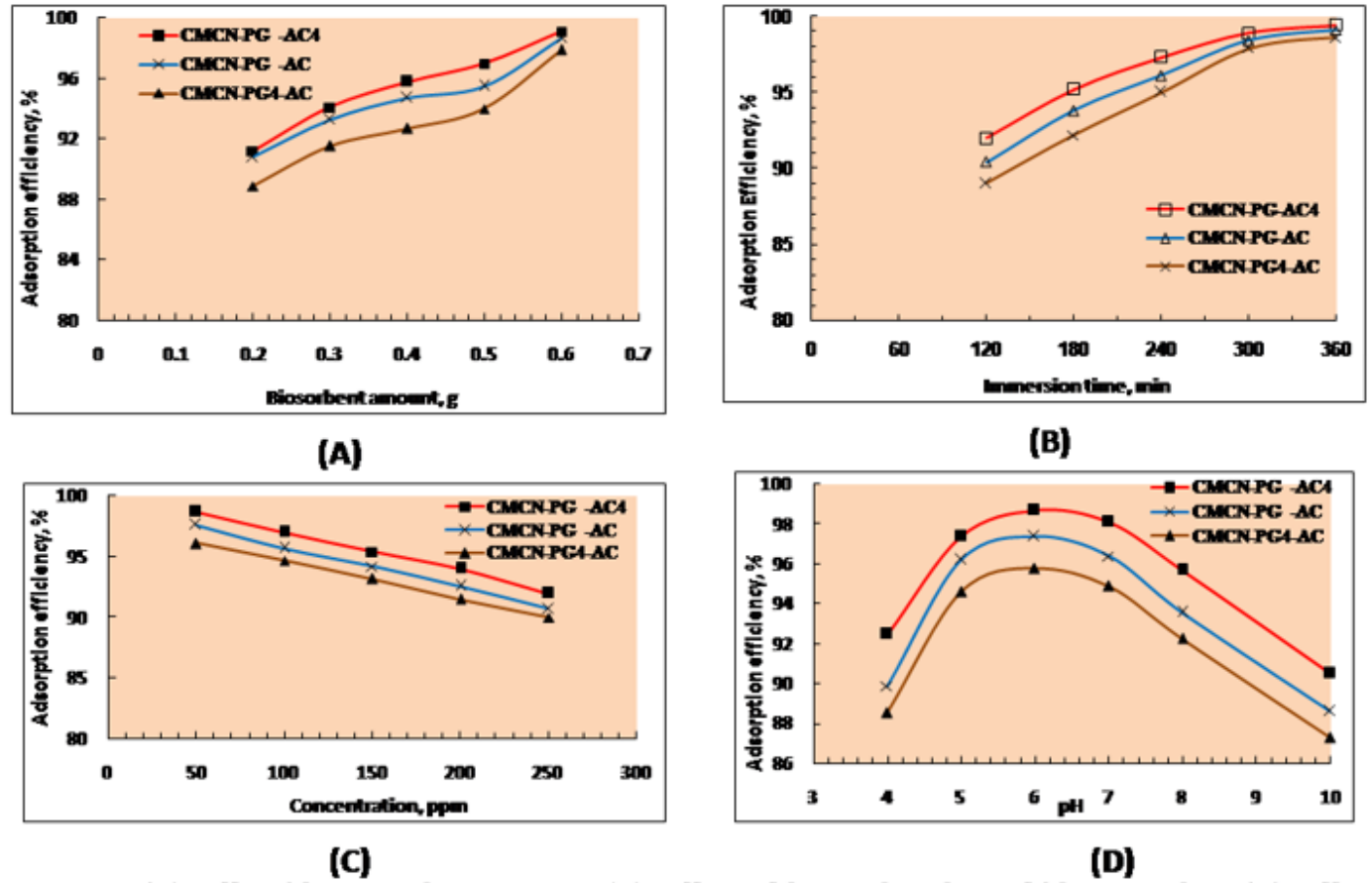

Figure 2: (A) Effect biocomposites amounts, (B) Effect of immersion time of biocomposites, (C) Effect of initial Cr^{3+} metal ion concentration , and (D) Effect of pH of the medium on the adsorption efficiency of Cr^{3+} metal ions.

Figure 2

See image above for figure legend

Image not available with this version

Figure 3

Legend not provided with this version

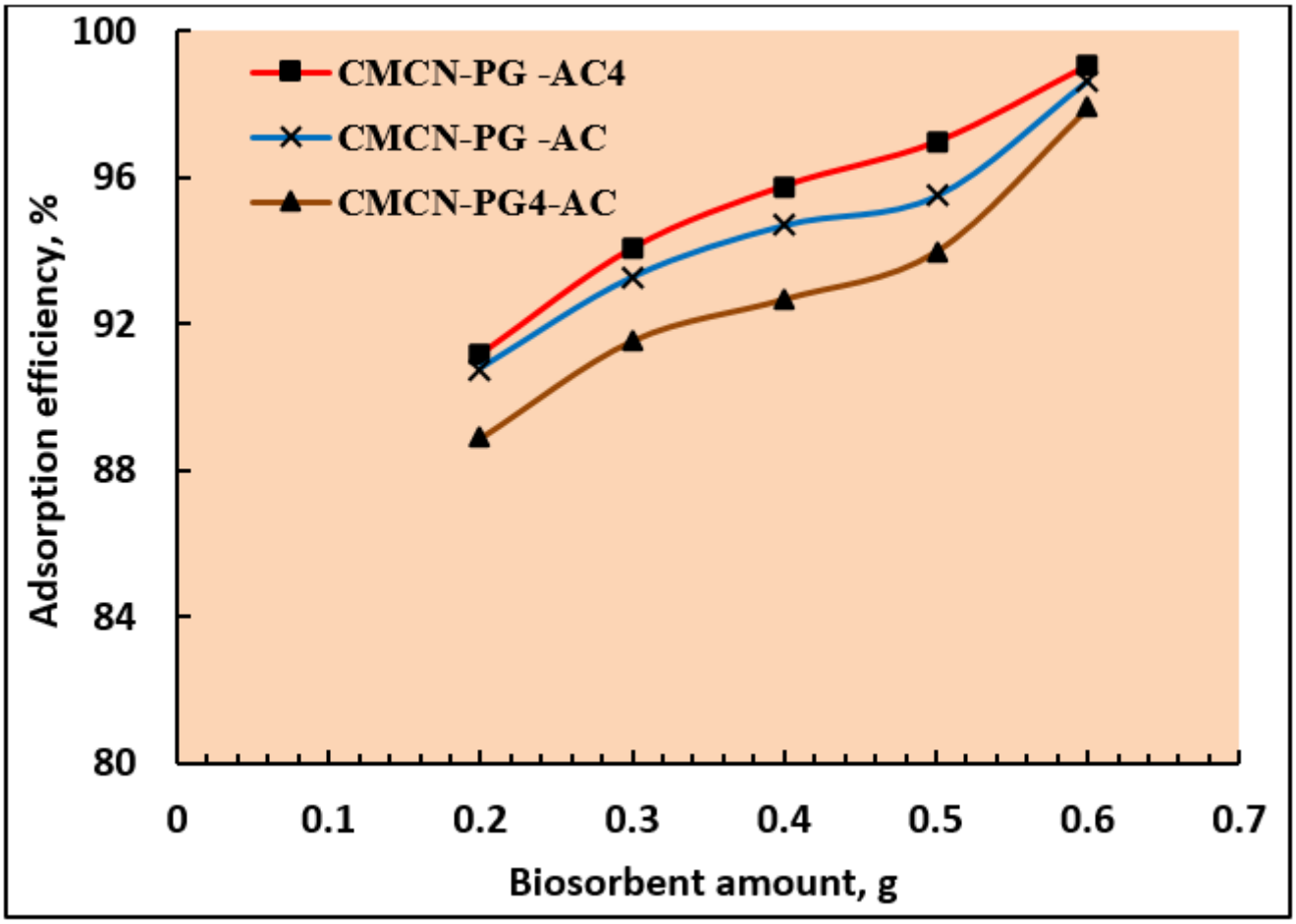

Figure 4

Effect of CMCN-PG-AC4, CMCN-PG-AC, and CMCN-PG4-AC biocomposites amounts on the adsorption efficiency of Cr^{3+} metal ions.

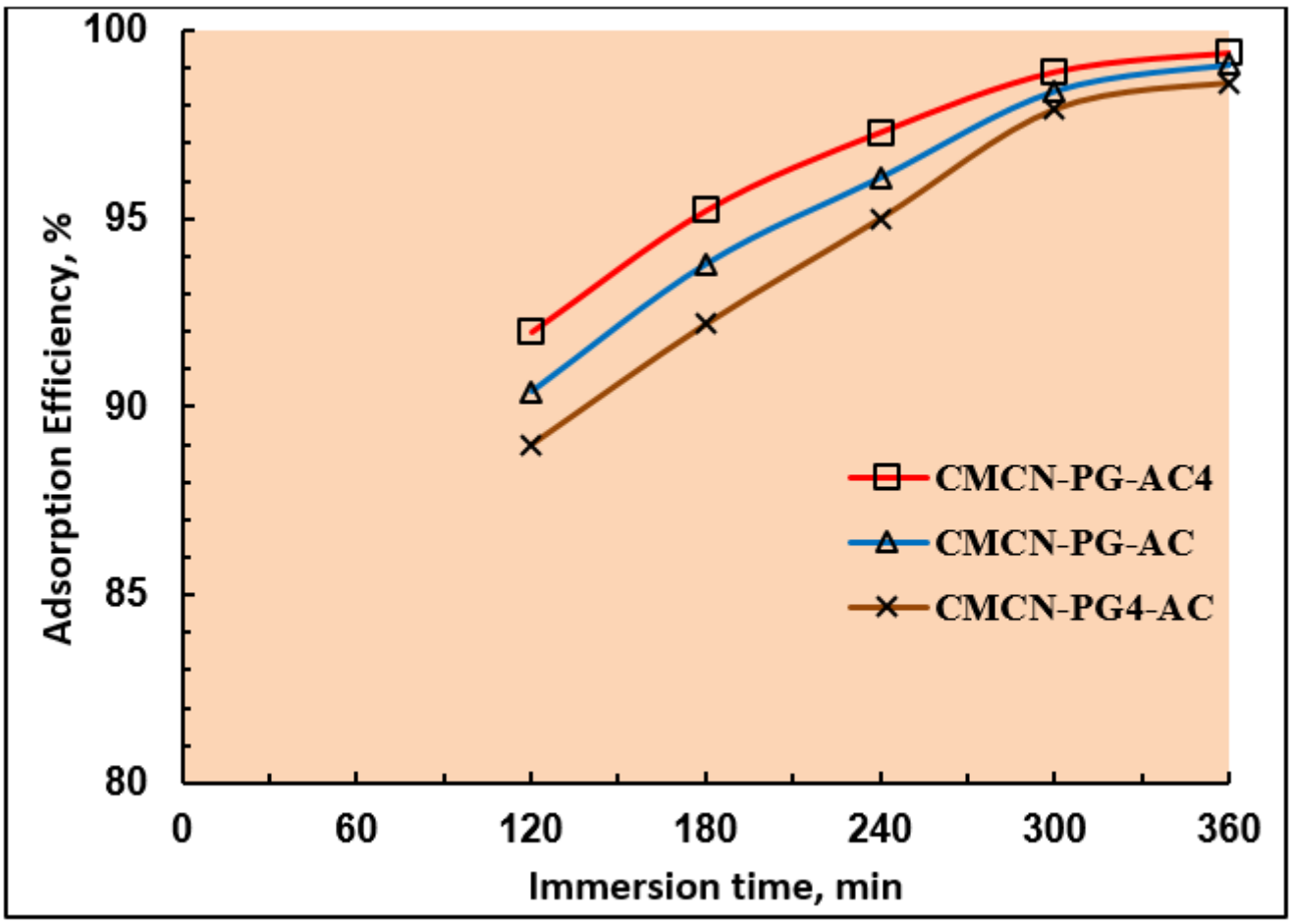

Figure 5

Effect of immersion time of CMCN-PG-AC4, CMCN-PG-AC, and CMCN-PG4-AC biocomposites on the adsorption efficiency of Cr^{3+} metal ions.

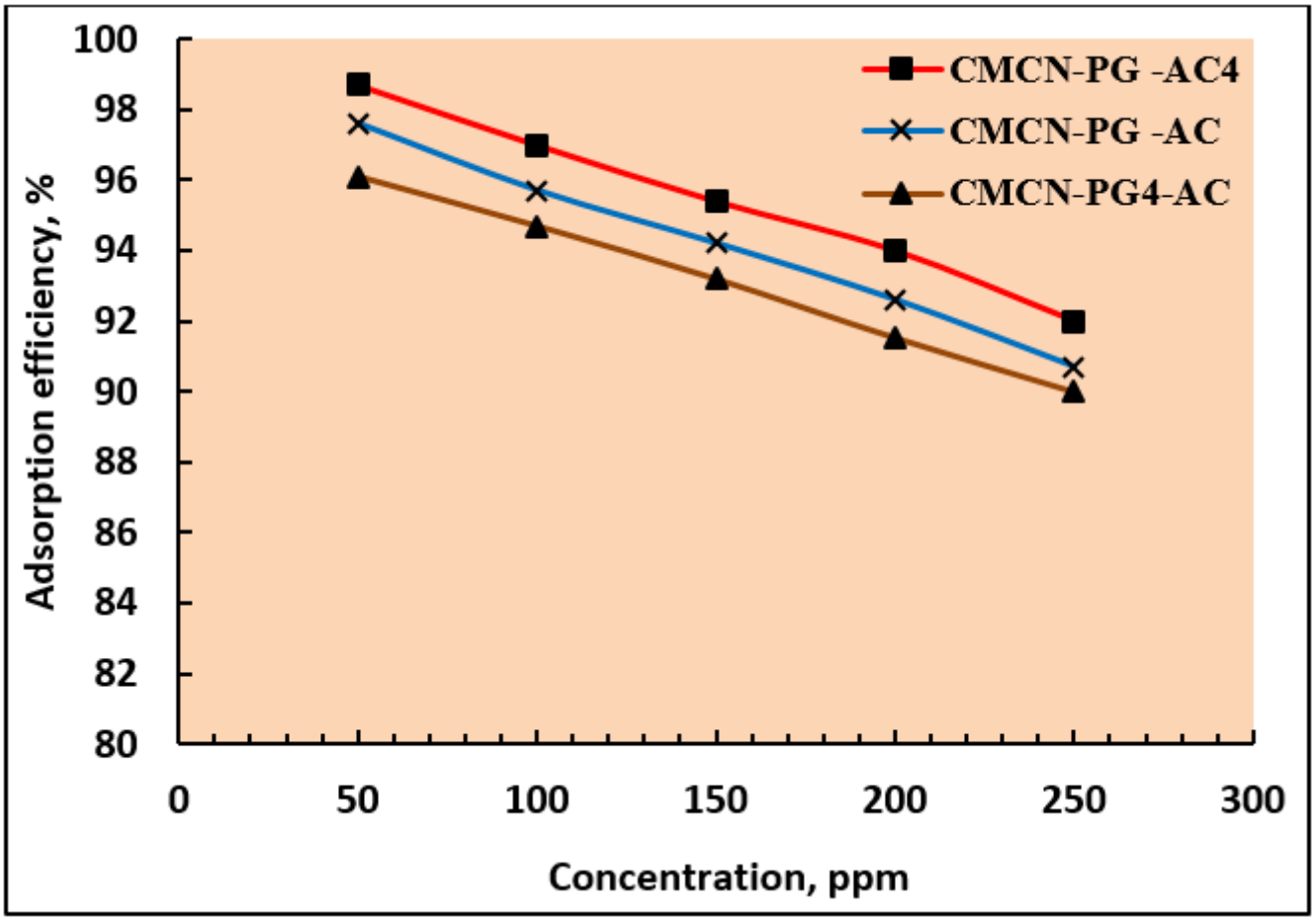

Figure 6

Effect of initial Cr^{3+} metal ion concentration on the adsorption efficiency of CMCN-PG-AC4, CMCN-PG-AC, and CMCN-PG4-AC biocomposites.

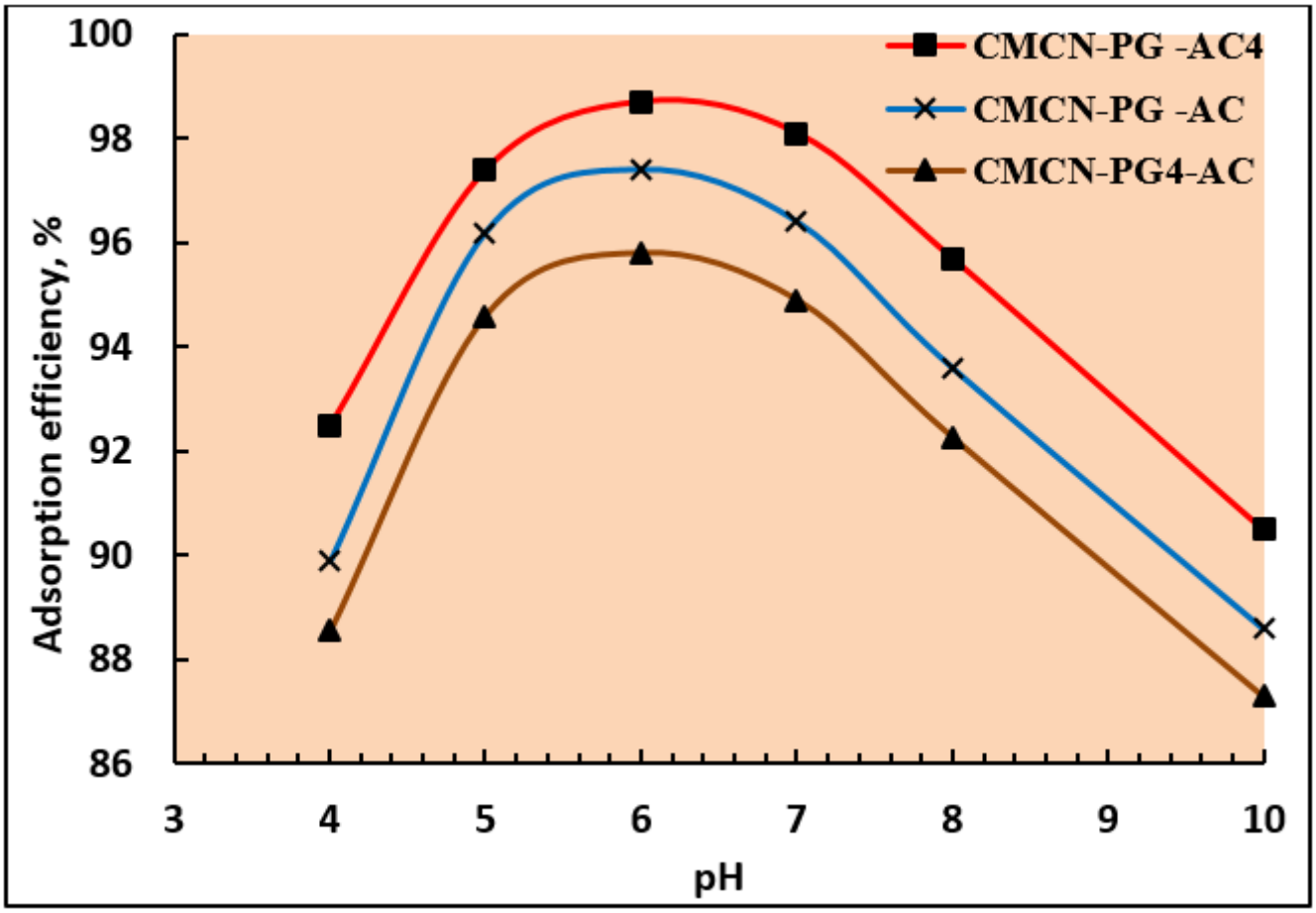

Figure 7

Effect of pH of the medium on the adsorption of Cr^{3+} metal ion using CMCN-PG-AC4, CMCN-PG-AC, and CMCN-PG4-AC biocomposites.

Figure 8

Langmuir adsorption isotherm presentation of the adsorption process of Cr^{3+} onto CMCN-PG-AC4, CMCN-PG-AC, and CMCN-PG4-AC biocomposites.

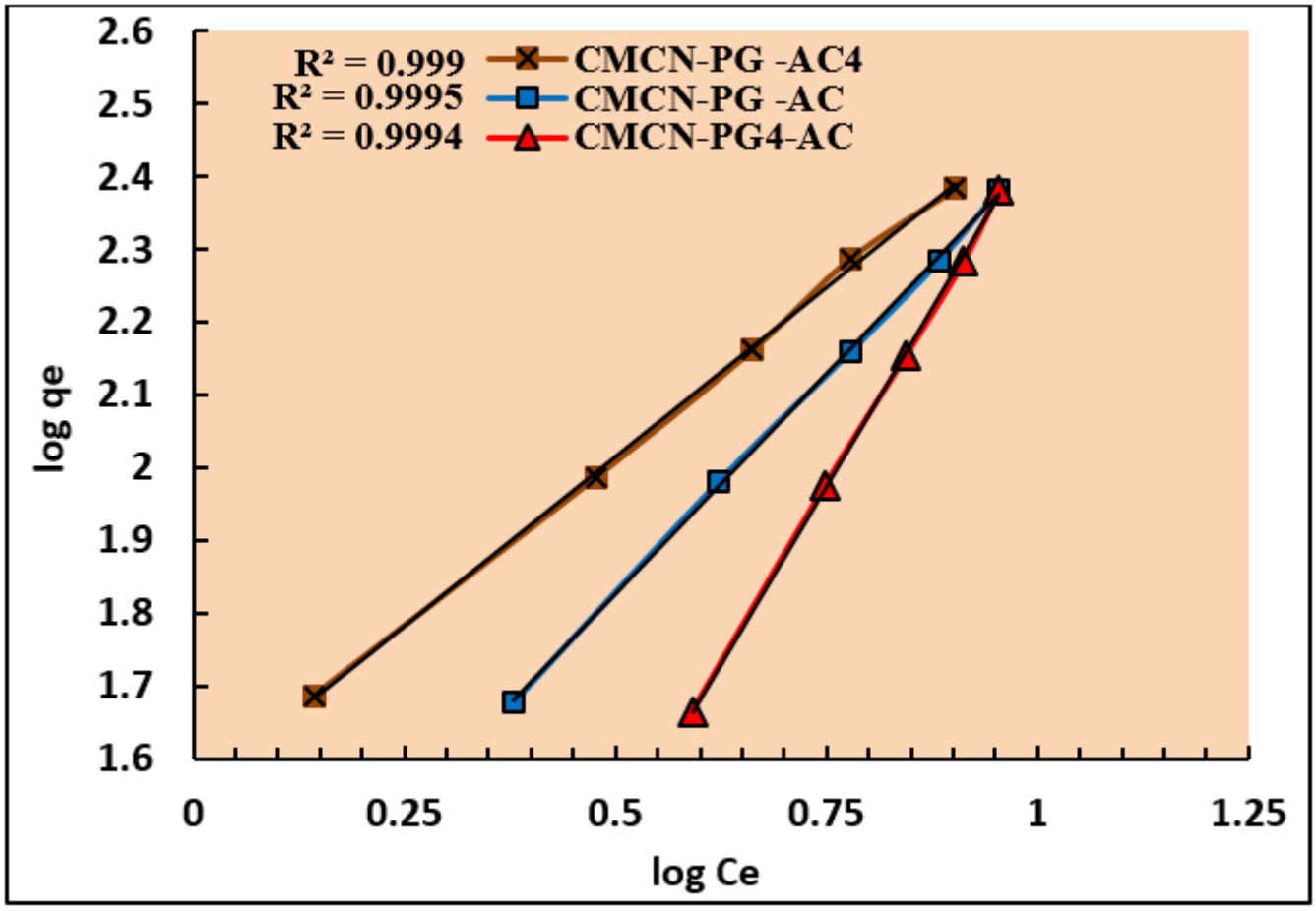

Figure 9

Freundlich adsorption isotherm presentation of the adsorption process of Cr^{3+} onto CMCN-PG-AC4, CMCN-PG-AC, and CMCN-PG4-AC biocomposites.

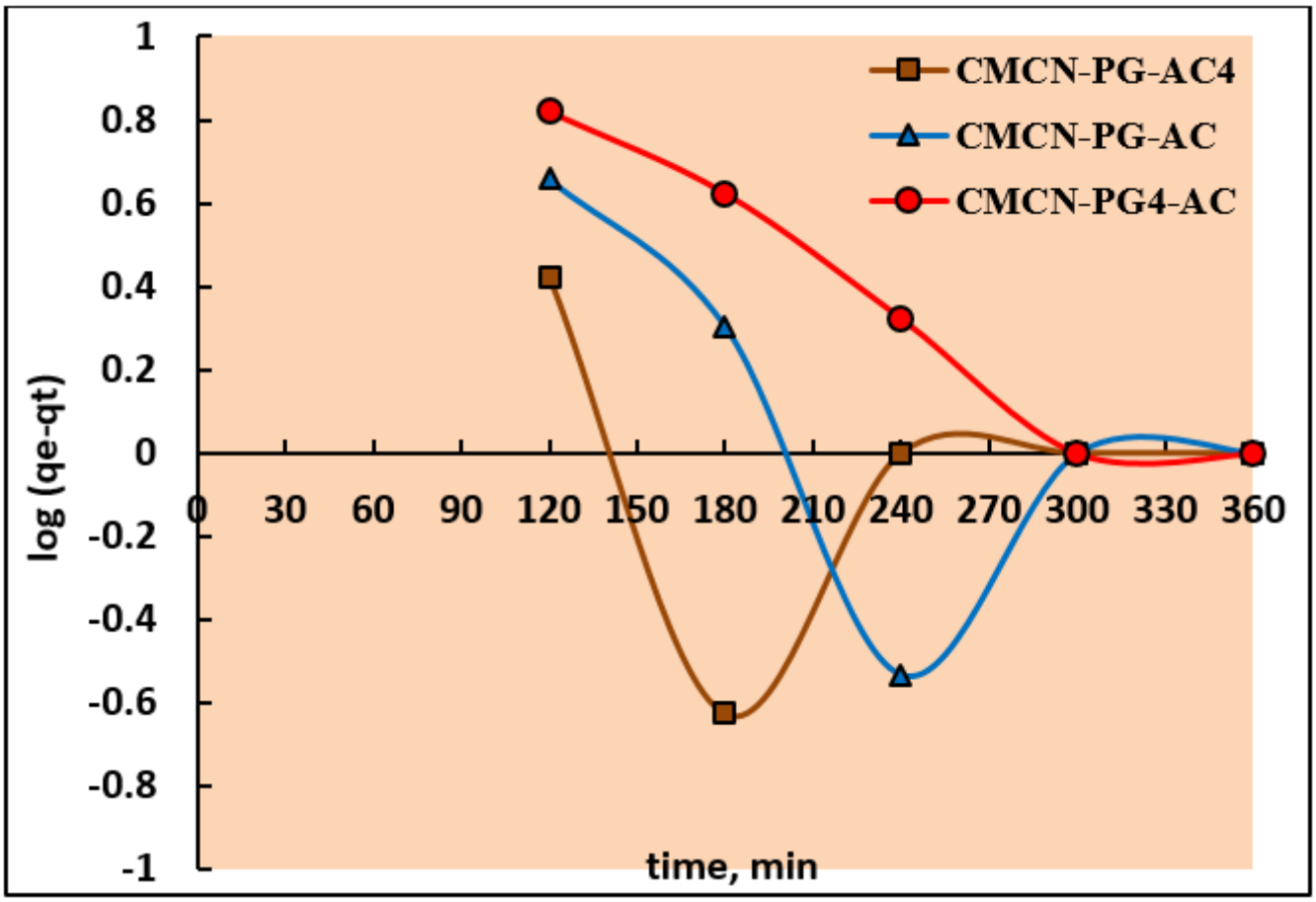

Figure 10

Fitting data of Cr^{3+} adsorption on CMCN-PG-AC4, CMCN-PG-AC, and CMCN-PG4-AC biocomposites according to Pseudo-first order kinetic model.

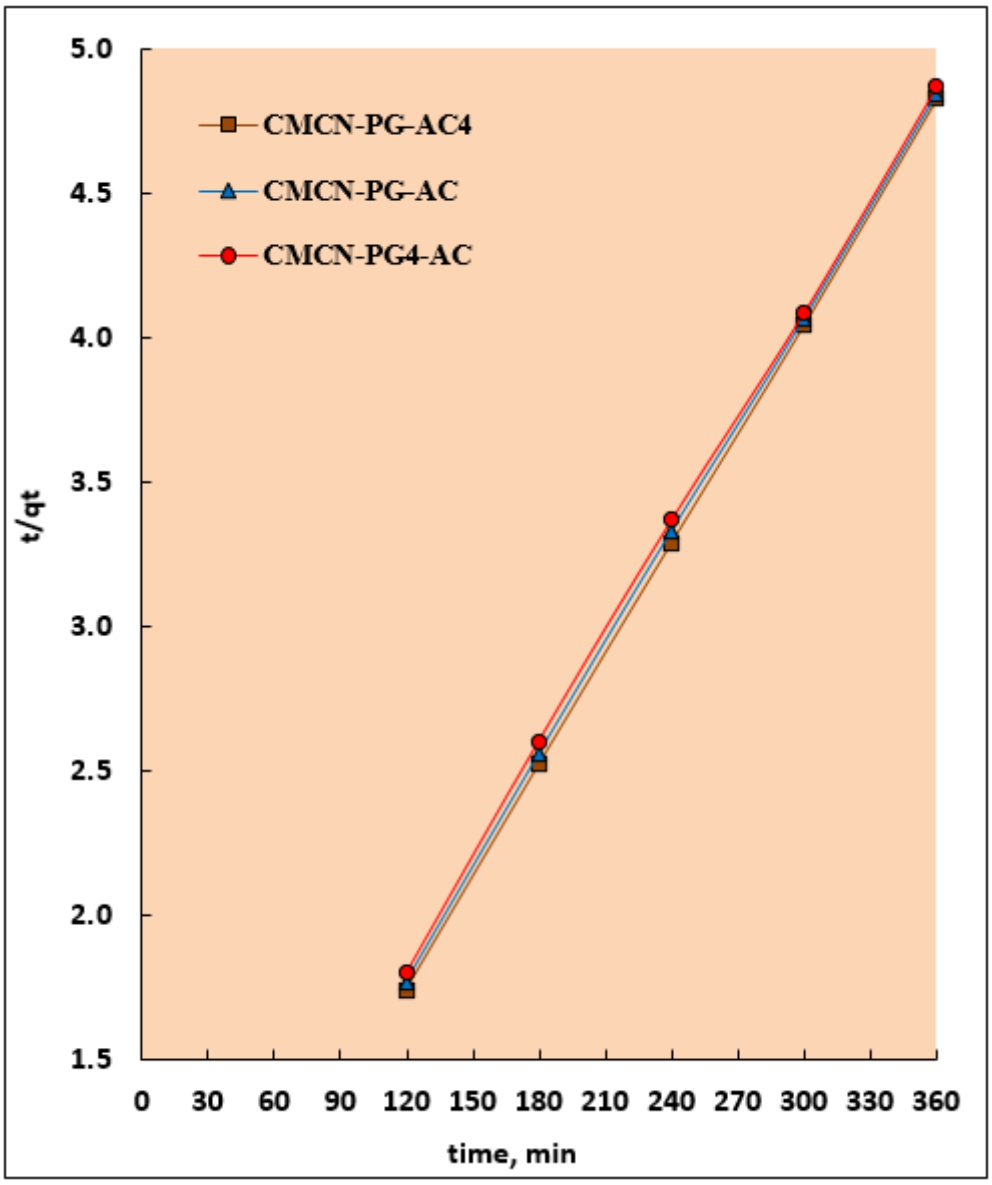

Figure 11

Presentation of adsorption data using pseudo-second-order kinetic model.

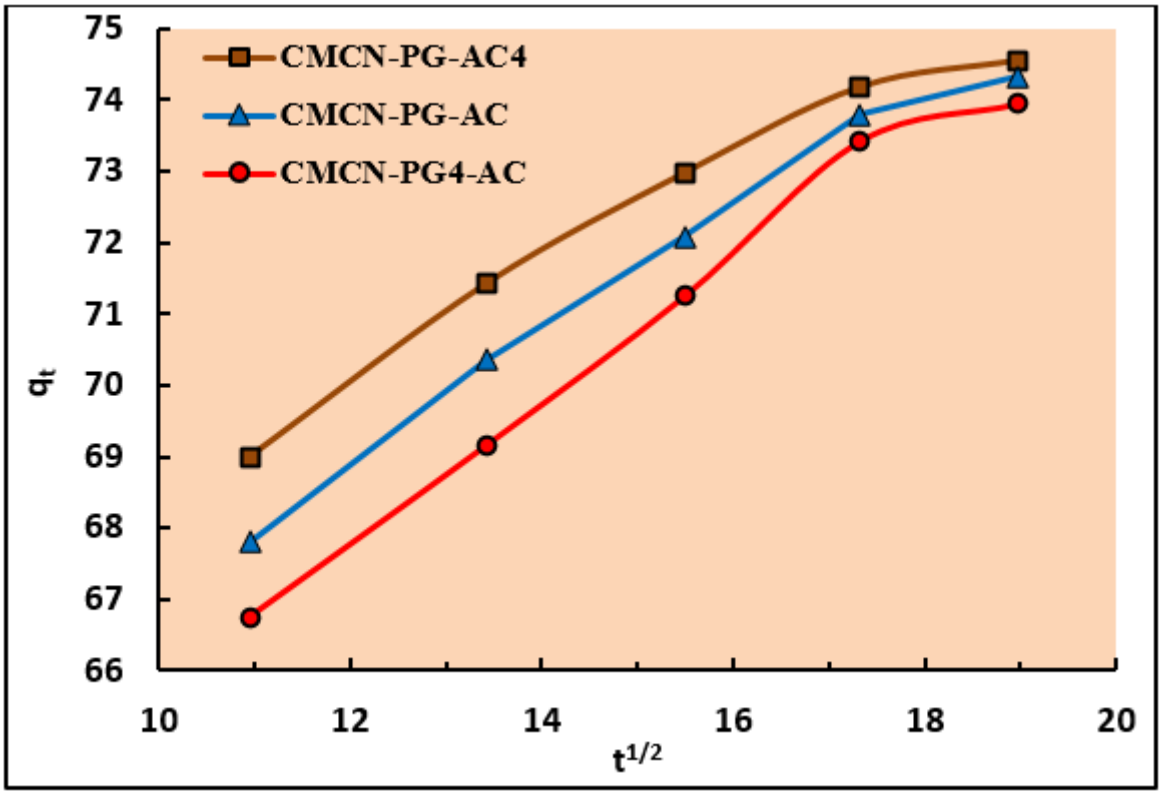

Figure 12

Interpretation of experimental adsorption data using intraparticle diffusion model.

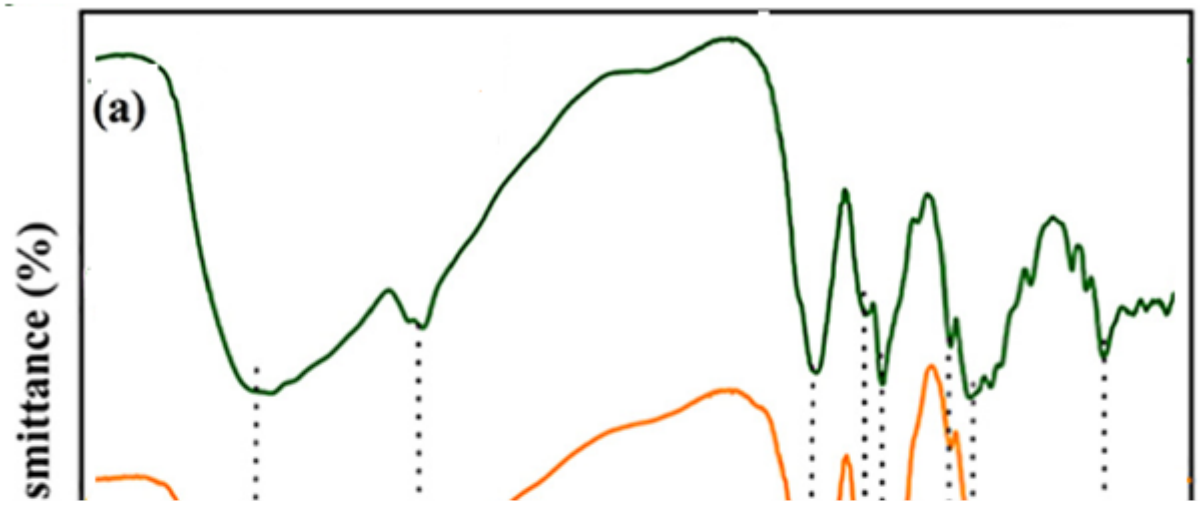

Figure 13

FTIR spectrum of CMCN-PG-AC4 biocomposite before and after adsorption process of Cr(III) ions .

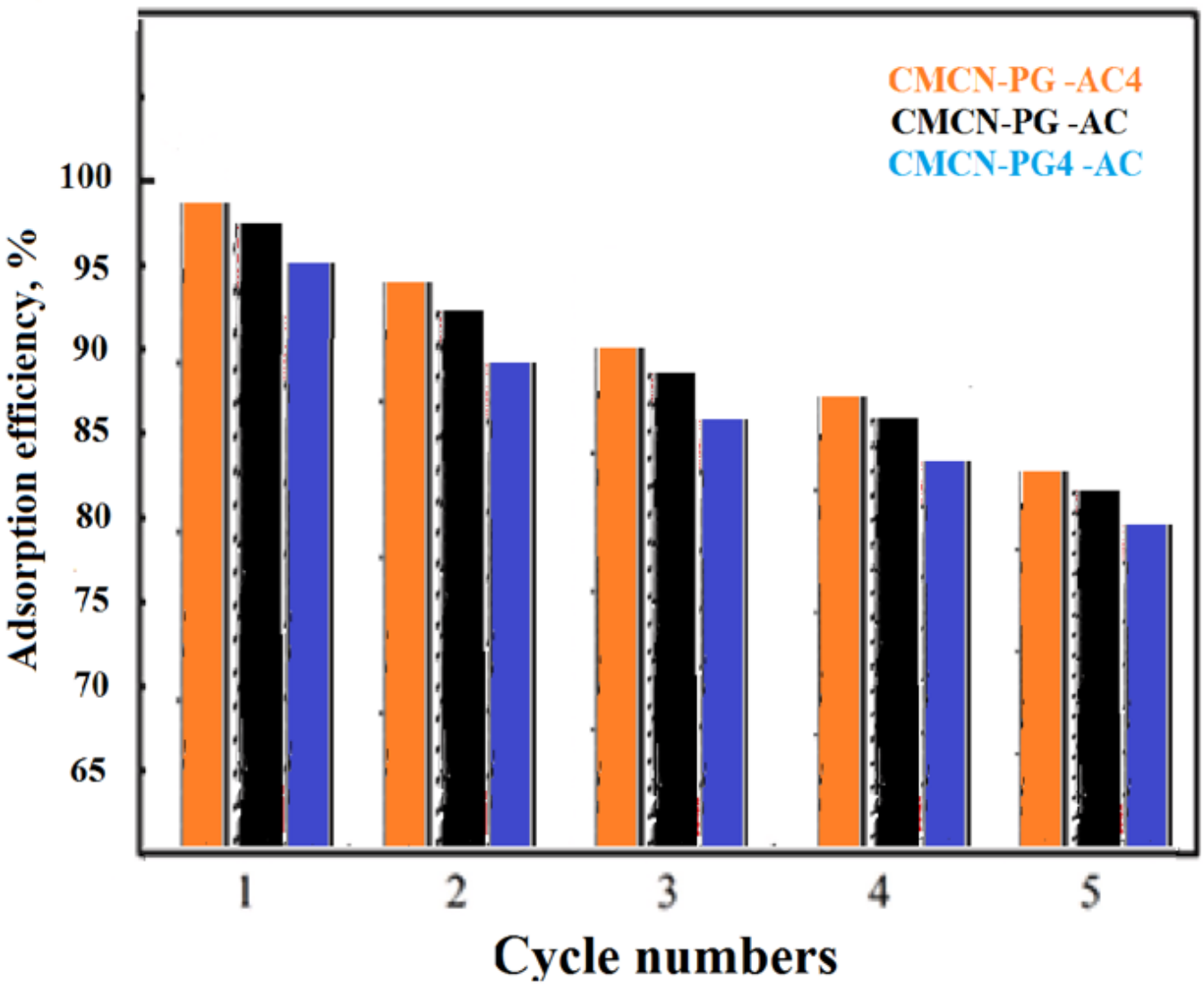

Figure 14

Reusability studies of CMCN-PG-AC4, CMCN-PG-AC, and CMCN-PG4-AC biocomposites in the adsorption process of Cr^{3+} metal ion.

Supplementary Files

This is a list of supplementary files associated with this preprint. Click to download.

- scheme.png